*Progress In Electromagnetics Research C, Vol. 114, 57–67, 2021*

# A Novel Miniaturized L-Band Filter with Great Stopband Characteristics Using Interdigitated Coupled Lines CRLH-TL Structure

**Peng Wang[1], Kaiyue Duan[2, *], Minquan Li[2], Man Zhang[2], and Baokun Jin[2]**

**Abstract**—This paper proposes a novel bandpass filter for L-band based on CRLH TL, which is mainly formed by coupling a high-pass characteristic module with a low-pass characteristic module in a cascade. The high-pass module consists of an interdigitated coupled line and a grounding via, owning to its singular characteristics, which the miniaturization is realized. The low-pass module is composed of a C-type resonator with high-low impedance lines, which can realize great sideband attenuation characteristics. To further improve its out-of-band rejection characteristics, a complementary split-ring resonator (CSRR) defective ground structure with single-pole attenuation characteristics is loaded, and a transmission zero is introduced at $2.5f_0$ out-of-band. The test results are in great agreement with the simulation ones, and the dimensions are only $0.20\lambda_g * 0.22\lambda_g$. Compared with other similar types, the filter proposed in this paper has miniaturization, great passband selection characteristics, stopband characteristics, and the advantage of low insertion loss.

## 1. INTRODUCTION

In wireless communication system, the filter with frequency selection function directly affects the whole communication system, microwave engineering and communication field of filter miniaturization, easy integration, stopband rejection, insertion loss, passband selectivity, and wireless communication system has put forward stringent requirements [1–3]. In 1968, Veselago proposed the concept of left-handed material [4], which was later experimentally verified by Pendry et al. to have exotic properties such as negative refractive index [5]. Composite right/left-handed transmission line (CRLH TL) is a novel artificial electromagnetic material with backward wave propagation characteristics, negative phase velocity, zero order, negative resonance, and other exotic properties, which are widely used in filter design and are beneficial for achieving microwave devices with miniaturization, new structures, and high performance [6–10]. In [11], a novel methodology bandpass filter was proposed based on the coupled simplified composite right/left-handed (SCRLH) zeroth-order resonators to realize miniaturization. In [12], a coplanar waveguide loaded modified split-ring resonator was proposed, which was connected to the ring using open-ended microstrip stubs to improve response characteristics and achieve great passband selection characteristics. In [13], a compact ultra-wideband bandpass filter consisting of a T-shaped resonator and two CPW transition structures with different complementary split ring resonators was proposed, which achieved high suppression and narrow stopband with miniaturized and flat group time delay. In [14], a via-less wideband bandpass filter with the bandwidth of 90% and group delay of 0.22 ns in the passband was implemented by introducing a closed rectangular ring resonator, interdigital capacitors, curved current lines, and semi-circular short nodes. In [15], a differential bandpass filter with

*Received 11 May 2021, Accepted 23 June 2021, Scheduled 19 July 2021*
* Corresponding author: Kaiyue Duan (2508009688@qq.com).
[1] Anqing Normal University, Anqing 246011, China. [2] Key Lab of Ministry of Education of Intelligent Computing & Signal Processing, Anhui University, Hefei 230601, China.

dual-band response is implemented based on a substrate integrated waveguide loaded with CSRR, which has the advantage of miniaturization and low insertion loss. Above all, the purpose of this paper is to propose a filter that satisfies the design requirements with low production cost, new miniaturized structure, great passband rejection, and wide stopband characteristics.

This paper proposes a miniaturized non-resonant CRLH TL bandpass filter based on the theoretical analysis of CRLH TL using its unique singular characteristics. Firstly, the CRLH resonant unit module with high-pass characteristics is proposed, on the basis of which a low-pass module with low-pass attenuation characteristics is introduced. Then, the bandpass filter is implemented by coupling the high-pass module and low-pass module in cascade. Among them, the high-pass module consists of interdigitated coupled lines with grounding vias, and the CRLH resonant resonators are smaller in size than conventional $\lambda/4$ resonators when working in the left-hand region, realizing filter miniaturization. The low-pass module is formed by a C-type resonator with low-pass attenuation characteristics consisting of high-low impedance lines. Finally, the out-of-band rejection is improved by etching a low-pass single-pole attenuation characteristic CSRR defective ground structure on the floor to achieve great stopband characteristics. The bandpass filter proposed in this paper works in L-band and has miniaturization, great passband selection characteristics as well as stopband characteristics, and has some value for engineering applications.

## 2. DESIGN AND ANALYSIS

### 2.1. CRLH High-Pass Module

A CRLH resonant cell with high-pass characteristics is proposed. The left-hand cell consists of interdigitated coupled lines series capacitor $C_L$ and a grounded shunt inductor $L_L$, and the right-hand cell consists of a voltage gradient causing parasitic capacitance $C_R$ and the parasitic inductance $L_R$ caused by the flow of current on the metal surface. The basic structure of the resonator and its equivalent circuit are shown in Figs. 1(a) and (b). The dimensions of the structure parameters are shown in Table 1.

**Table 1.** High-pass resonant unit parameters dimensions (unit: mm).

| $f$ | $g$ | $e$ | $la$ | $r1$ | $d2$ |
|---|---|---|---|---|---|
| 0.5 | 1.0 | 1.5 | 12.5 | 0.5 | 1.4 |

Based on empirical formulas, the values of series capacitance $C_L$ and shunt inductance $L_L$ of the left-hand unit can be calculated as shown in the following equations [16, 17].

$$L_L \approx \frac{z_0}{\omega}\tan\left(\beta^l\right) \tag{1}$$

$$C_L \approx (\varepsilon_r + 1)\, l\, [(N-3)A_1 + A_2]\ (\text{pF}) \tag{2}$$

$$Z_0 = Z_L = \sqrt{L_L/C_L} \tag{3}$$

$$A_1 = 4.409\tanh\left[0.55\left(\frac{h}{w}\right)^{0.45}\right]10^{-6}\,(\text{pF}/\mu\text{m}) \tag{4}$$

$$A_2 = 9.92\tanh\left[0.52\left(\frac{h}{w}\right)^{0.5}\right]10^{-6}\,(\text{pF}/\mu\text{m}) \tag{5}$$

$\beta$ is the propagation constant at the center frequency point, $l$ the interdigital length, $w$ the interdigital width, and $h$ the thickness of dielectric substrate.

To verify this approach, the bandpass filter is simulated and implemented on a 1.575 mm-thick Rogers Ro5880 substrate which has a loss tangent of 0.0009 and relative dielectric constant $\varepsilon_r$ of 2.2. The simulation results are shown in Fig. 1(c): It has great passband characteristics from 1.6 GHz to 3 GHz; the insertion loss is 0.2 dB; the return loss is better than 15 dB; and the stopband rejection is

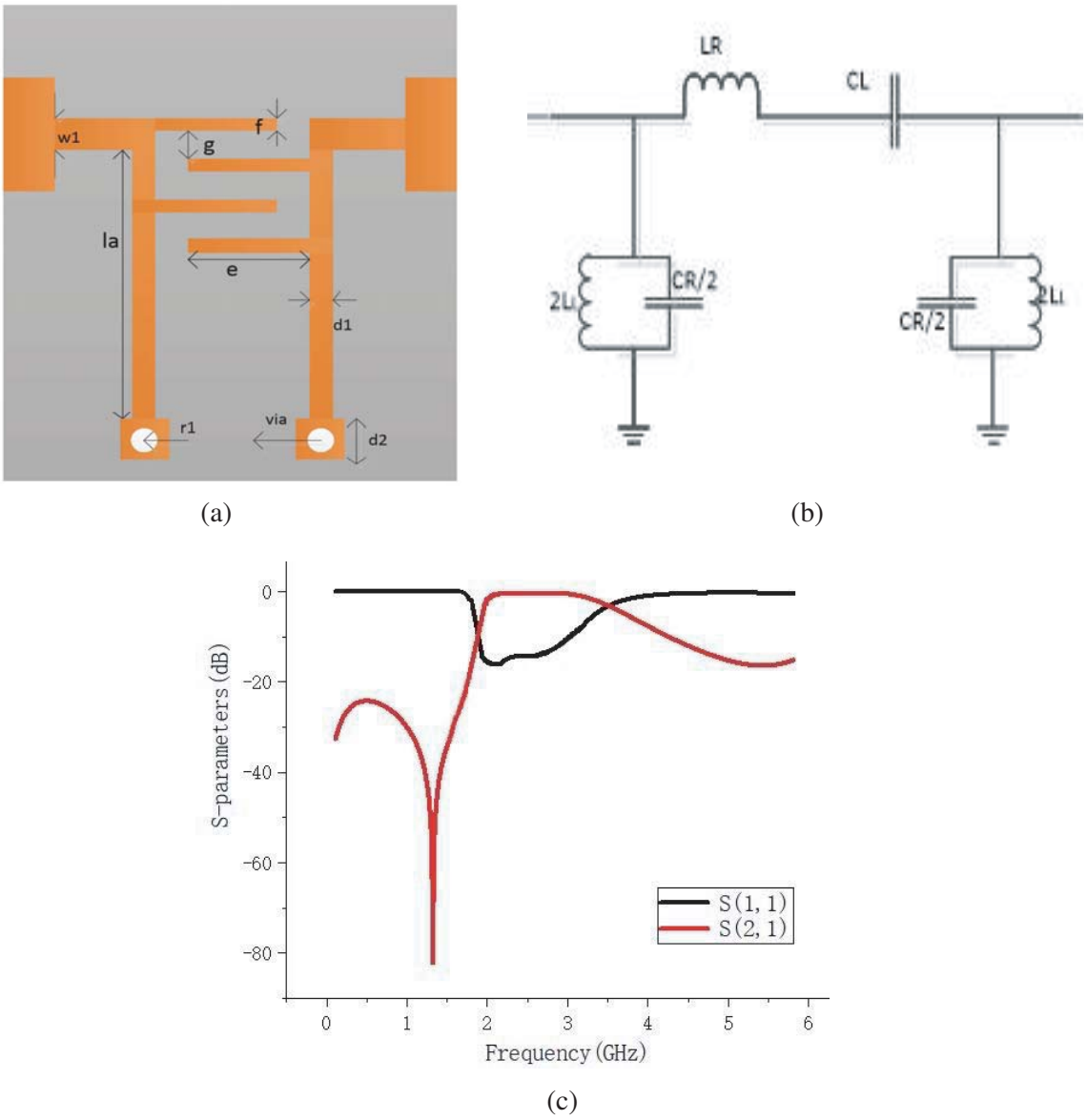


**Figure 1.** (a) Structure of the CRLH resonator. (b) Equivalent circuit. (c) Simulation curve.

83 dB at 1.35 GHz, which fully shows that the CRLH resonant unit proposed in this paper has excellent high-pass characteristics.

### 2.2. Low-Pass Module

The low-pass module is a C-shaped resonator with low-pass attenuation characteristics composed of a high-low impedance line structure, which can be equated to an RLC circuit, as shown in Fig. 2.

In the RLC equivalent circuit, there are relations $Z_0 = Z_L$, $Y = \frac{1}{R} + j[\omega c - \frac{1}{\omega L}]$, with $Z_0$ for the port impedance value. When the RLC circuit resonates with $Z = 1/Y = R$, the value of $R$ is obtained as:

$$R = 2Z_0 \left( \frac{1}{2Z_0/\left(2Z_0 + Z\right)} - 1 \right) \Big/ f = f_c \tag{6}$$

$f_c$ is the resonant frequency, with $f_c = 1/(2\pi\sqrt{LC})$, $Q = \omega_c CR$, $BW = f_c/Q$, then the values of $C$ and

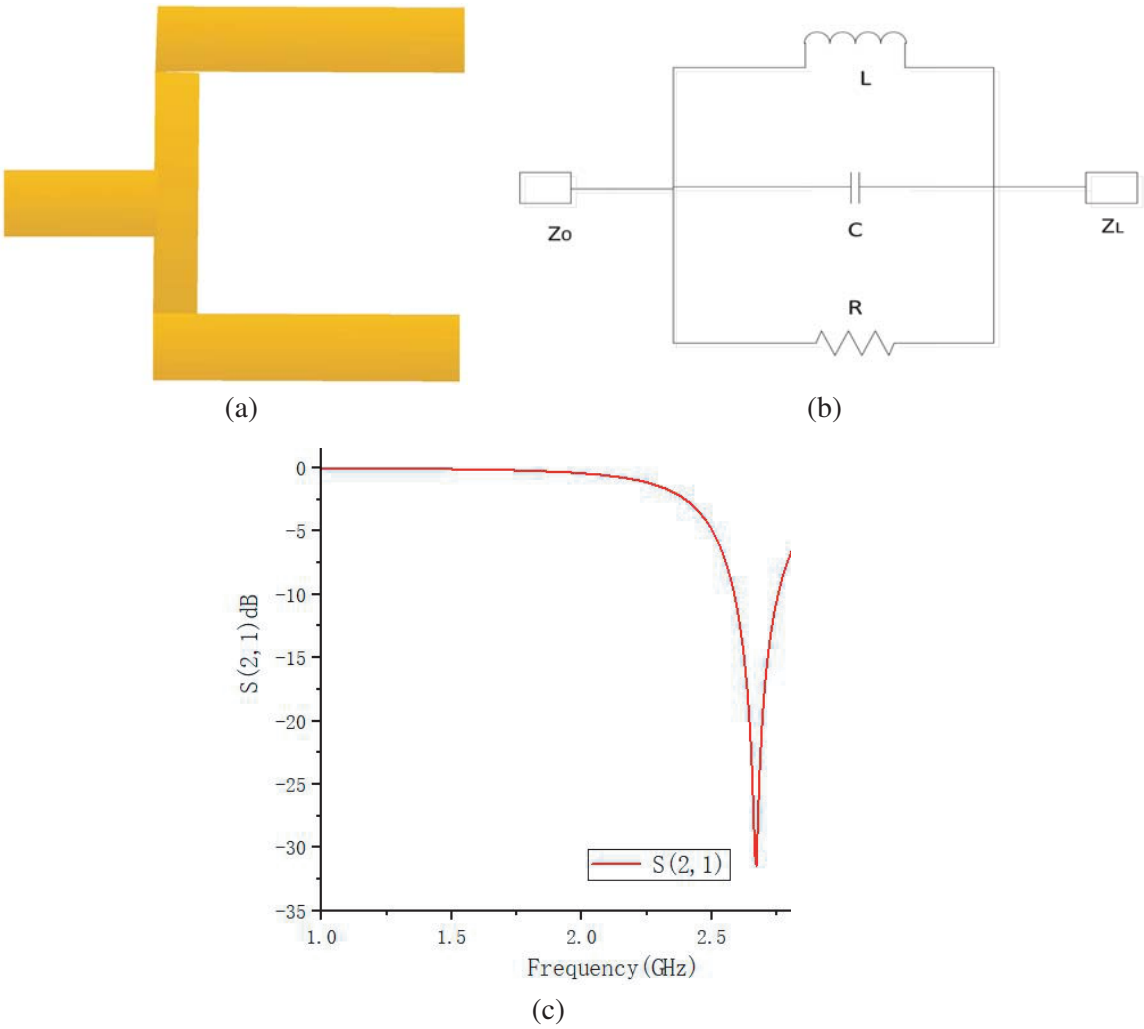


**Figure 2.** (a) Structure of the high pass module. (b) Equivalent circuit. (c) Simulation curve.

$L$ are obtained from the relation.

$$C = 1/(2\pi R * BW) \tag{7}$$

$$L = 1/\left(4\pi^2 f_c^2 * C\right) \tag{8}$$

According to the project requirements of this paper, the value of $f_c$ is $-31$ dB, and the BW of $-20$ dB is 60 MHz. There are formulas to calculate the initial value of the equivalent circuit: $C = 3.22$ pF, $R = 3825.97\,\Omega$, $L = 1.104$ nH. In order to verify the correctness of the equivalent circuit design, simulations are performed using ADS software, and the simulation results are shown in Fig. 3(c). The simulation results fully verify that the low-pass module has great sideband attenuation characteristics and is an important module for the bandpass filter propose in this paper.

### 2.3. Design of Bandpass Filter

In this paper, the propose of the CRLH TL bandpass filter is to realize the CRLH TL bandpass filter by coupling the high-pass module to the low-pass module in cascade. The coupling between the high-pass and low-pass modules is adjusted so that the passband frequency works in the corresponding L-band. The structure is shown in Fig. 3(a), and the simulation curve is shown in Fig. 3(b). The structural dimensions are shown in Table 2.

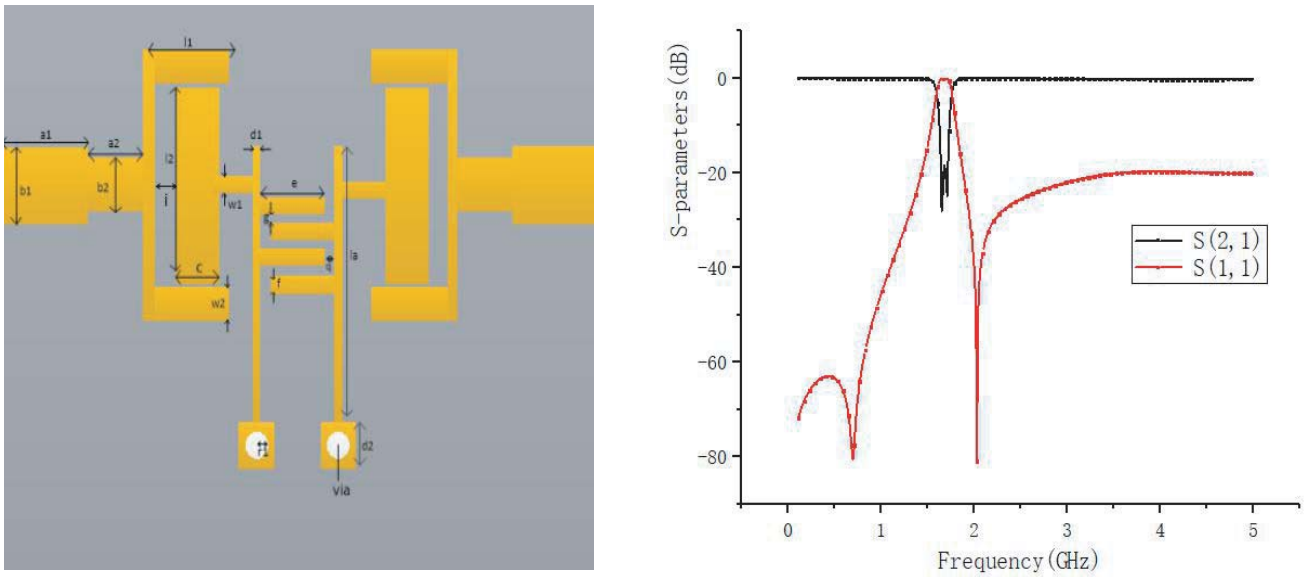


(a) (b)

**Figure 3.** (a) Bandpass filter structure. (b) Simulation curve.

**Table 2.** Bandpass filter parameters dimensions (unit: mm).

| Parameter table (unit:mm) | | | | | |
|---|---|---|---|---|---|
| $a1$ | 3.1 | $a2$ | 1.9 | $l1$ | 4.4 |
| $la$ | 13.6 | $d2$ | 1.4 | $l2$ | 7.2 |
| $c$ | 1.5 | $w2$ | 1.1 | $g$ | 0.1 |

The simulation results show that the bandpass filter cutoff frequency is from 1.68 GHz to 1.82 GHz, which is applied to the L-band. The zeros of suppression system are better than 80 dB on both sides of the passband; the left skirt selection characteristic is 87.5 dB/GHz; and the right skirt selection characteristic is 380.95 dB/GHz achieving great passband selection characteristics.

### 2.4. Improved Bandpass Filter

The presence of higher harmonics and spurious signals causes the filter to have less than great out-of-band rejection. Therefore, the stopband characteristics are improved without affecting the passband. Low-pass filters are commonly used for the suppression of high harmonics and spurious signals. Although the traditional high-low impedance line filters can suppress high harmonics well, they require high order to meet the requirements and are not beneficial to miniaturization. In this paper, we introduce a CSRR defective ground structure to achieve great out-of-band rejection of the filter with further miniaturization by using its low-pass single-pole attenuation characteristics [18, 19], as shown in Fig. 4.

According to the equivalent circuit, the value of the equivalent capacitance of CSRR defective ground structure can be introduced by Equation (9), and the value of the equivalent inductance can be introduced by Equation (10). The structure dimensions are shown in Table 3.

$$C = \frac{\omega_c}{2 * Z_0} \frac{1}{\omega_0^2 - \omega_c^2} \tag{9}$$

$$L = \frac{1}{\omega_0^2 C} = \frac{1}{4\pi^2 f_0^2 C} \tag{10}$$

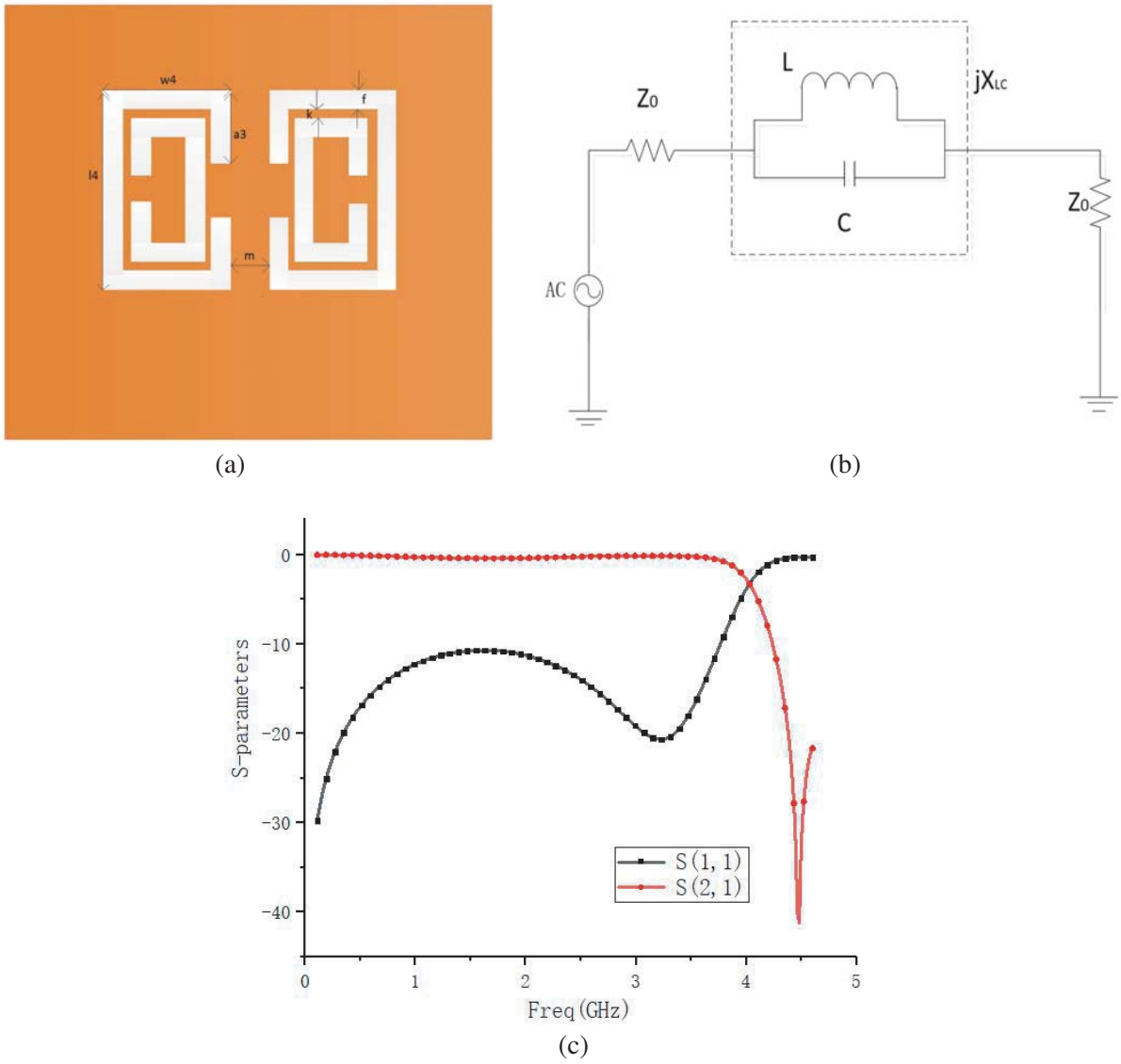


**Figure 4.** (a) CSRR structure. (b) Equivalent circuit. (c) Attenuation curve.

**Table 3.** CSRR defective ground structure parameters dimensions (unit: mm).

| $l4$ | $w4$ | $a3$ | $m$ | $k$ | $f$ |
|---|---|---|---|---|---|
| 9.8 | 4.3 | 2.9 | 4.1 | 0.1 | 0.6 |

$\omega_c$ is the cut-off angle frequency; $Z_0$ is the standard impedance value, and let it be 50 Ω.

The simulation results in Fig. 4(c) show that the CSRR defective ground structure has obvious low-pass attenuation characteristics out-of-band, with significant suppression at the 1.82 GHz cutoff frequency, and $S_{21}$ is relatively flat in the passband, which is better than 2 dB.

The CSRR defective ground structure is loaded into the proposed filter, and the final proposed bandpass filter structure in this paper is shown in Fig. 5(a). The simulation results are shown in Fig. 5(b). The cut-off frequency is from 1.68 GHz to 1.82 GHz, which works in L-band; the return loss is better than 22.1 dB and the insertion loss better than 0.25 dB; there is an attenuation pole

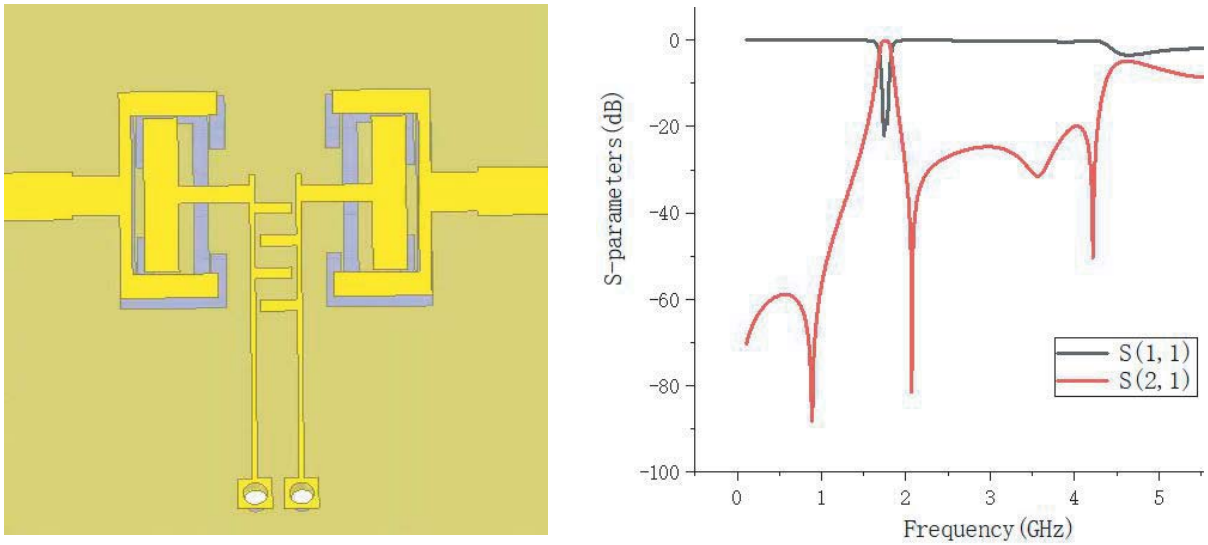


(a) (b)

**Figure 5.** (a) Load CSRR bandpass filter structure. (b) Simulation curve.

**Table 4.** Comparison of various bandpass filter.

| Reference | stopband-width | $RL$ (dB) | $IL$ (dB) | size ($\lambda_g * \lambda_g$) | $TZs$ (dB) |
|---|---|---|---|---|---|
| [20] | $1.64f_0$ | 21.8 | 0.65 | $2.40 * 1.64$ | 35 |
| [21] | $2.72f_0$ | 17.0 | 0.96 | $1.19 * 0.54$ | 72 |
| [22] | $2.02f_0$ | 10.0 | 1.35 | $0.57 * 1.45$ | 38 |
| [23] | $1.40f_0$ | 18.8 | 1.20 | $0.62 * 0.62$ | 40 |
| [24] | $1.50f_0$ | 19.8 | 1.70 | $0.79 * 0.06$ | 50 |
| [25] | $1.71f_0$ | 14.8 | 1.60 | $0.40 * 0.35$ | 70 |
| [26] | $1.46f_0$ | 26.3 | 0.61 | $0.08 * 0.11$ | 49 |
| This work | $2.50f_0$ | 22.1 | 0.25 | $0.20 * 0.22$ | 83 |

with 50 dB out-of-band suppression at 4.5 GHz, and the structure size is $0.2\lambda_g * 0.22\lambda_g$. The proposed filter has miniaturization, low insertion loss, great passband selection characteristics, and stopband characteristics. In order to further show the advantages of the proposed filter in this paper, the performance comparison of vaious filters is summarized in Table 4.

## 3. MEASUREMENT AND ANALYSIS

In order to verify the feasibility of the filter proposed in this paper, physical processing and testing were carried out, and the results are shown in Fig. 6, which shows that the test results are in great agreement with the simulation. The test results show that the filter return loss is better than 20 dB, insertion loss better than 2 dB, and the structure size is only $0.2\lambda_g * 0.22\lambda_g$, while it provides great passband selection characteristics and stopband characteristics. Due to mismatching tolerance and parasitic effect of soldering, the return loss and insertion loss become worse than simulation result. Although the measurement results are a little different from simulation, it is acceptable.

To verify the existence of a negative refractive index region for the filter proposed in this paper, the $S$ parameter inversion is performed to extract the equivalent refractive index [27, 28]. Based on the impedance in Equation (11), the refractive index expression (12) is introduced, and then the inversion

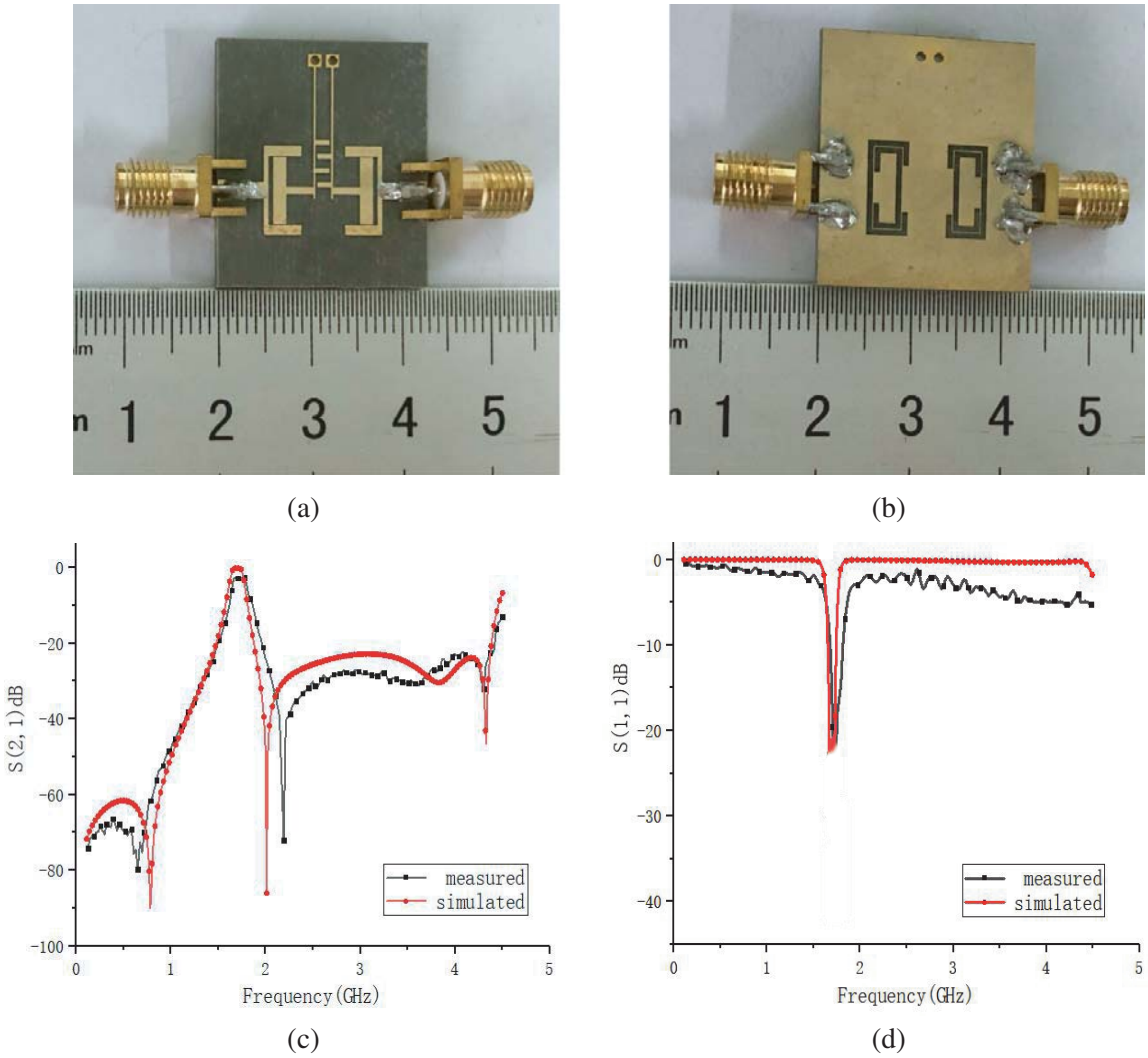


**Figure 6.** (a) (b) Physical processing front and back. (c) (d) Measurement results $S$-parameters.

is performed using Matlab in conjunction with $S$-parameters.

$$Z = \pm\sqrt{\frac{(1+S_{11})^2 - S_{21}^2}{(1-S_{11})^2 - S_{21}^2}} \tag{11}$$

$$n = \frac{1}{kd}\left[\left\{\left[\ln\left(\frac{S_{21}}{1-S_{11}\dfrac{Z-1}{Z+1}}\right)\right] + 2m\pi\right\} - i\left[\ln\left(\frac{S_{21}}{1-S_{11}\dfrac{Z-1}{Z+1}}\right)\right]\right] \tag{12}$$

$$\varepsilon = n/z, \quad \mu = nz \tag{13}$$

From Equation (13), it can be seen that when the refractive index $n$ is negative, the permittivity and permeability are negative at the same time. $k = \omega_0/c$, $d$ is the maximum length of the unit element, and $m$ is the branch due to the periodicity of the sinusoidal function.

As shown in Fig. 7, the extracted equivalent refractive index curve demonstrates that the refractive index is negative within 2 GHz of the frequency band, fully confirming that the L-band bandpass filter proposed in this paper has left-handed material transmission characteristics.

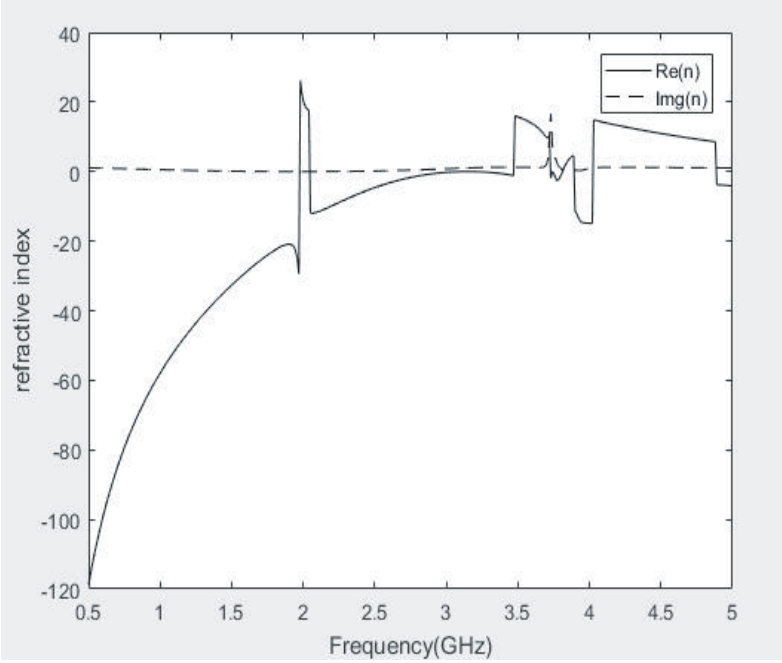


**Figure 7.** Equivalent refractive index curve.

## 4. CONCLUSION

In this paper, a bandpass filter has been proposed based on CRLH TL which works in the L-band. The bandpass filter design is realized by coupling cascade of a high-pass module with a low-pass harmonic module. In order to improve its out-of-band rejection characteristics, a great stopband characteristic is realized by loading a CSRR defective ground structure with low-pass single-pole attenuation characteristics. Through simulation and testing, which verifies the correctness of the filter proposed in this paper, it demonstrates miniaturization, great passband selection characteristics, and stopband characteristics compared with other similar works, and also has the advantage of low insertion loss. It is worthy of application in engineering.

## ACKNOWLEDGMENT

This work is supported by the Key Natural Science Research Project of Anhui Higher Education.

Institutions: Research on Environmental RF Energy Harvesting System KJ2019A0804, and the Key Projects of Natural Science Research in Anhui Universities KJ51477001.

## REFERENCES

1. Wang, C.-X., F. Haider, X. Gao, et al., "Cellular architecture and key technologies for 5G wireless communication networks," *IEEE Communications Magazine*, Vol. 52, No. 2, 122–130, 2014.
2. Chu, C. and X. Liao, "Modeling of an 8–12 GHz receiver front-end based on an in-line MEMS frequency discriminator," *Solid State Electronics*, Vol. 144, No. 7, 54–59, 2018.
3. Hong, J. S., "Microstrip filters for RF/microwave applications," *IEEE Microwave Magazine*, Vol. 3, No. 3, 62–65, 2002.
4. Veselago, V. G., "The electrodynamics of substances with simultaneously negative values of $\varepsilon$ and $\mu$," *Physics-Uspekhi*, Vol. 10, No. 4, 509–514, 1968.

5. Pendry, J., B. Holden, et al., "Magnetism from conductors and enhanced nonlinear phenomena," *IEEE Transactions on Microwave Theory & Techniques*, Vol. 47, No. 11, 2075–2084, 1999.
6. Smith, D. R., W. J. Padilla, D. C. Vier, et al., "Composite medium with simultaneously negative permeability and permittivity," *Physical Review Letters*, Vol. 84, No. 18, 4184–4178, 2000.
7. Eleftheriades, G. V., A. K. Iyer, and P. C. Kremer, "Planar negative refractive index media using periodically L-C loaded transmission lines," *IEEE Transactions on Microwave Theory & Techniques*, Vol. 50, No. 12, 2702–2712, 2002.
8. Keshavarz, S. and N. Nozhat, "Dual-band Wilkinson power divider based on composite right/left-handed transmission lines," *13th International Conference on Electrical Engineering/Electronics, Computer, Telecommunications and Information Technology (ECTI-CON)*, 2016.
9. Keshavarz, S., R. Keshavarz, and A. Abdipour, "Compact active duplexer based on CSRR and interdigta loaded microstrip coupled lines for LTE application," *Progress In Electromagnetics Research C*, Vol. 109, 27–37, 2021.
10. Keshavarz, S., A. Abdipour, A. Mohammadi, et al., "Design and implementation of low loss and compact microstrip triplexer using CSRR loaded coupled lines," *AEU — International Journal of Electronics and Communications*, Vol. 111, 152913–152913, 2019.
11. Gong, J. Q. and Q. X. Chu, "Miniaturized microstrip bandpass filter using coupled SCRLH zeroth-order resonators," *Microwave & Optical Technology Letters*, Vol. 51, No. 12, 2985–2989, 2009.
12. Sanz, V., A. Belenguer, L. Martinez, et al., "Balanced right/left-handed coplanar waveguide with stub-loaded split-ring resonators," *IEEE Antennas and Wireless Propagation Letters*, Vol. 65, No. 13, 193–196, 2014.
13. Chu, Q.-X., J.-Q. Huang, et al., "Compact ultra-wideband filter with dual notched bands based on complementary split ring resonators," *Microwave and Optical Technology Letters*, Vol. 52, No. 11, 2509–2512, 2010.
14. Choudhary, D. K. and R. K. Chaudhary, "Vialess wideband bandpass filter using CRLH transmission line with semi-circular stub," *International Conference on Microwave and Photonics (ICMAP)*, 1–2, 2015.
15. Zhang, H., W. Kang, and W. Wu, "Miniaturized dual-band differential filter based on CSRR-loaded dual-mode SIW cavity," *IEEE Microwave and Wireless Components Letters*, Vol. 28, No. 10, 897–899, 2018.
16. Iyer, A. K. and G. V. Eleftheriades, "Negative refractive index metamaterials supporting 2-D waves," *IEEE MTT-S International Microwave Symposium Digest*, Vol. 2, No. 10, 1067–1070, 2002.
17. Wu, Y. M., "Design of phase-shifter using composite right-left handed transmission line," *Journal of Antennas*, Vol. 06, No. 4, 61–69, 2017.
18. Park, J.-I., et al., "Modeling of a photonic bandgap and its application for the low-pass filter design," *Asia Pacific Microwave Conference*, Vol. 2, No. 10, 331–334, 1999.
19. Ahn, D., J. S. Park, C. S. Kim, et al., "A design of the low-pass filter using the novel microstrip defected ground structure," *IEEE Transactions on Microwave Theory & Techniques*, Vol. 49, No. 1, 86–93, 2001.
20. Gómez-García, R., J. Muñoz-Ferreras, D. Psychogiou, et al., "Balanced symmetrical quasi-reflectionless single-and dual-band bandpass planar filters," *IEEE Microwave and Wireless Components Letters*, Vol. 28, No. 9, 798–800, 2018.
21. Jones, T. R. and M. Daneshmand, "Miniaturized slotted bandpass filter design using a ridged half-mode substrate integrated waveguide," *IEEE Microwave and Wireless Components Letters*, Vol. 29, No. 5, 334–336, 2016.
22. Luo, C., et al., "Quasi-reflectionless microstrip bandpass filters using bandstop filter for out-of-band improvement," *IEEE Transactions on Circuits and Systems II*, Vol. 1109, No. 10, 1849–1853, 2019.
23. Psychogiou, D. and R. Gómez-García, "Multi-mode-cavity-resonator-based bandpass filters with multiple levels of transfer-function adaptivity," *IEEE Acces*, Vol. 1109, No. 10, 24759–24765, 2019.

24. Chen, C., "A coupled-line coupling structure for the design of quasi-elliptic bandpass filters," *IEEE Transactions on Microwave Theory and Techniques*, Vol. 66, No. 4, 1921–1925, 2018.
25. Zhang, M., M. Li, K. Duan, et al., "A novel miniaturized bandpass filter basing on stepped-impedance resonator," *Progress In Electromagnetics Research Letters*, Vol. 97, 77–85, 2021.
26. Li, M. and K. D. Xu, "Miniaturized bandpass filter using E-stub loaded CRLH-TL resonator," *17th International Symposium on Communications and Information Technologies (ISCIT)*, 1–3, 2017.
27. Numan, A. B. and M. S. Sharawi, "Extraction of material parameters for metamaterials using a full-wave simulator [Education Column]," *IEEE Antennas and Propagation Magazine*, Vol. 55, No. 5, 202, 2014.
28. Ca Loz, C. and T. Itoh, "Transmission line approach of Left-Handed (LH) materials and microstrip implementation of an artificial LH transmission line," *IEEE Trans. Antennas & Propag.*, Vol. 52, No. 5, 1159–1166, 2004.